

# Preventing Personal Data Theft from Images with Adversarial Machine Learning

Thomas Cilloni

University of Mississippi  
Oxford, USA  
t.cilloni@go.olemiss.edu

Wei Wang

Xi'an Jiaotong-Liverpool University  
Suzhou, China  
wei.wang03@xjtlu.edu.cn

Charles Walter

University of Mississippi  
Oxford, USA  
cwwalter@olemiss.edu

Charles Fleming

University of Mississippi  
Oxford, USA  
fleming@olemiss.edu

**Abstract**—Facial recognition tools are becoming exceptionally accurate in identifying people from images. However, this comes at the cost of privacy for users of online services with photo management (e.g. social media platforms). Particularly troubling is the ability to leverage unsupervised learning to recognize faces even when the user has not labeled their images. This is made simpler by modern facial recognition tools, such as FaceNet, that use encoders to generate low dimensional embeddings that can be clustered to learn previously unknown faces. In this paper, we propose a strategy to generate non-invasive noise masks to apply to facial images for a newly introduced user, yielding adversarial examples and preventing the formation of identifiable clusters in the embedding space. We demonstrate the effectiveness of our method by showing that various classification and clustering methods cannot reliably cluster the adversarial examples we generate.

**Index Terms**—adversarial machine learning, facial recognition, privacy

## I. INTRODUCTION

The rapid rise of the Information Age has left a gap in the legal infrastructure protecting users' privacy. While there exist laws to protect the privacy of citizens in most countries around the world, these laws were designed for "analog" data, and are difficult to apply to digital data that can trivially be copied, shared, or even stolen. Even in cases where laws do exist, for example, the European Union General Data Protection Regulation[1], it is difficult to enforce when data can be transferred to other legal jurisdictions. Image data is particularly concerning because of its invasive applications and the lack of protection from these practices in existing laws [2]. Because of the lack of policies to defend people's digital privacy rights, it is necessary for users to protect themselves where other protection measures are not in place.

We focus on a common feature in many online services: photo tagging. Most consumer applications that provide services for the storage and distribution of images, such as Facebook and Flickr, make use of facial recognition tools [3]. We propose a tool for users to protect their privacy by masquerading the most personally identifiable feature of an individual: the face. Such protection is offered through a system that alters images in a manner that is indistinguishable to human eye, and yet large enough to hinder the effectiveness of facial recognition software.

In order to build this system, we take existing adversarial machine learning techniques designed for classifiers and

modify them for the context of generators of embeddings for facial images. We explore combinations of parameters and strategies to search for the best cloaking algorithm for the proposed tool. In doing so, we show how adversarial machine learning methods can be adapted to different neural network architectures. Finally, we find optimum schemes and sets of parameters for assessing the representational power of a neural network, regardless of whether adversarial ML strategies are applied or not.

Our contributions are as follows:

- 1) We explore novel ways to port existing adversarial machine learning methods to networks that generate embeddings and use *triplet loss* to calculate the cost.
- 2) Given the results obtained in the previous exploratory study, we propose a facial privacy tool that is able to render faces unrecognizable by facial recognition tools while keeping the alterations undetectable to humans.
- 3) We test our system against various verification, identification, and recognition tasks while evaluating the representational power of facial image embeddings with the availability of increasingly large and deep datasets.

## II. LITERATURE REVIEW

### A. Facial Recognition

By definition, facial identification is a classification task. Classification, however, allows only a fixed number of output classes in the network, which is quite impractical for facial recognition, as a new network would have to be designed and trained every time a new person was to be identified. The solution is to transition from a classification task to a more regression-like task with networks that generate meaningful representations of faces in the form of numerical vectors.

Siamese neural networks, sometimes referred to as twin neural networks, are the most direct implementation of the concept of computing embeddings for classification purposes. They were first introduced in 1994 for the verification of hand-written signatures [4], but only recently have they gained popularity, especially in computer vision. These networks are called *siamese* because they are actually made of two neural networks that share weights and operate concurrently. [5] explains clearly how this structure works in practice to calculate the similarity between two faces: given two face images  $I_1$  and

$I_2$ , and using a Siamese network of convolutional networks  $G$  with a weight vector  $W$ , the similarity  $E$  between the two faces can be calculated as in Eq. 1.

$$E_W(I_1, I_2) = \|G_W(I_1) - G_W(I_2)\| \quad (1)$$

The currently most advanced face identification model, FaceNet [6], was first proposed by Google in 2015. This model introduces a new lightweight strategy to identify faces: a deep CNN trained directly to optimize the representation of a face described as a 128-dimensional numerical vector. Among the major contributions of FaceNet is the definition of a new metric for the cost function: triplet loss. Older models compute the loss by looking at the difference between the expected and the computed similarity between faces' embeddings. Examples include DeepFace, which uses Cross-Entropy Loss [7][8], and the series of DeepId, which use Cross-Entropy Loss alone and together with Euclidean Loss[9][10][11][12]. Triplet loss, instead, uses triplets of faces' images: an anchor  $a$  with identity  $ID$ , a positive example  $p$  also with identity  $ID$ , and a negative example  $n$  with identity  $ID' \neq ID$ . The loss is calculated relative to each triplet of images (or to each triplet of embeddings) as to how close the anchor is to the negative sample and how distant it is from the positive sample. Eq. 2 formalizes the cost function  $J$  of the triplet loss with margin  $m$  and  $A$ ,  $P$ , and  $N$  being the sets of anchors, positive and negative examples, respectively. The margin defines how different should the anchor-positive and anchor-negative distances be in order to have a loss of 0 for that triplet.

$$J(W, m) = \sum_i (\max(E_W(A^i, P^i) - E_W(A^i, N^i) + m, 0)) \quad (2)$$

## B. Adversarial Machine Learning

Adversarial Machine Learning is a relatively new area of study in artificial intelligence that looks at how neural networks can be fooled by feeding them deceptive inputs [13]. The techniques studied in adversarial machine learning are cyber attacks by nature, and can be divided into two categories based on the resources available to the attacker: *white-box* and *black-box*. Our interest is in the first category. When an adversary has access to the cost function of the victim model, or to the victim model as a whole, the attack is of *white-box* type. Specifically, in computer vision, there exist a few thoroughly tested strategies to carry out *white-box* attacks.

The *Fast Gradient Sign Method* (FGSM) is one of the earliest examples of such algorithms. It was proposed in 2004 in research by Goodfellow et al. [14] and applied to neural networks for the classification of images, such as in DeepFool [15]. The algorithm consists in computing the gradient of the loss function for the given NN model, calculated using an image  $I$  as input, and then altering the fed image accordingly in order to maximize the loss. Specifically, by extending backpropagation to the input layer, it can be found how much each individual pixel in an image contributes to the loss. With this information, it becomes computationally easy to apply a

perturbation of small intensity  $\epsilon$  to maximize the loss. Eq. 3 defines how an adversarial example  $I'$  is generated using an image  $I$  with true class  $y$  fed to a model with cost function  $J$ .

$$I' = I + \epsilon * \text{sign}(\nabla_I J(\theta, I, y)) \quad (3)$$

An improvement over the simple FGSM is what is commonly referred to as *One-step Target Class* [16]. While FGSM simply decreases the confidence over the most likely target, the one-step target class method increases the confidence of a target class  $y' \neq y$ . This also decreases the confidence for  $y$ . Such a method is executed almost identically to the FGSM, with the target class in the cost function being  $y'$  instead of  $y$ , and the noise applied being subtracted instead of added.

Both the *One-step Target Class* and the *Fast Gradient Sign Method* are *one-shot* methods: they are executed only once. It is possible, however, to repeat this alteration process with small  $\epsilon$  to slowly bring an image to be misclassified. The *Basic Iterative Method* is the iterative equivalent of the FGSM as the *Iterative Least Likely Class* is to the *One-step Target Class*[17][18].

Shan et al. [19] propose *Fawkes*, a system to make faces in images unrecognizable by facial recognition tools. Its objective is almost identical to that of this paper: cloaking faces in images in an imperceptible way, yet enough to render them unidentifiable by common facial recognition systems. While the objective is the same, both the context and how this is achieved are significantly different.

The primary difference between *Fawkes* and our work is the type of neural networks treated, as the first analyzes and works with neural network *classifiers*. The larger and more diverse the dataset used is, the larger the applicability of the network becomes. However, the network is able to identify only as many people as it is originally designed to identify: it is impossible to classify the image of a person who was not included in the training dataset. This limitation is overcome by neural networks that perform feature extraction only, such as the one used in this paper. The two works are therefore applied to fundamentally different types of networks: classifiers and feature extractors.

Adversarial machine learning techniques have different effects on different types of neural networks. For example, the *Iterative Least Likely Class*, a method that performs very well on classifiers, shows weaker performances when applied to feature extractors, shown later. To mitigate this disadvantage we go beyond the single adversarial method proposed in *Fawkes* and investigate how different ones affect the efficacy of facial cloaking.

A final difference between the two pieces of research is the approach taken in cloaking images. In *Fawkes*, cloaking is evaluated by training facial image classifiers on cloaking images, and then checking the classification of uncloaked images. This paper proposes the opposite: using a network trained on uncloaked images, it is then checked if cloaked images can be identified or not. We believe this to be a better representation of real-world applications: in order to build a facial recognition network, a ML practitioner would use a dataset of labeled

face images and would not pick a dataset whose images have been altered with the goal of hindering classification. A few cloaked images can be effectively included in a dataset to train a network to be less vulnerable to adversarial examples, but using an entirely cloaked dataset is not desirable.

### III. SYSTEM DESIGN

Our goal is to devise a cloaking algorithm that can effectively render faces in images unidentifiable. In order to design such an algorithm, it is necessary to define what it means for a face to be cloaked.

The entire process of facial recognition can be summarized as follows: localization of the face in an image, isolation and (optional) alignment of the face, generation of the embedding of the image (feature extraction), and comparison of the embedding against a labeled dataset of known embeddings. The outcome of the last step is the identity of the face. The goal of the cloaking process is then to apply a very small alteration to a face in an image so that the face is misidentified in the last step. Identification, however, is a process for which multiple strategies exist. The DNN architectures used in facial cloaking attempt to generate very representative embeddings; how the embeddings are then used, specifically in the last step (identification), is up to the users of said architecture.

#### A. Algorithm

An embedding represents the characteristics of a face, but it is unknown what features correspond to which characteristics. What we can measure is the distance between embeddings that corresponds to the similarity (or dissimilarity) of the related faces. We then make the following hypothesis: cloaking for a face can be achieved by applying a noise mask such that the embedding of the resulting noisy face is distant to that of the unaltered face.

The crucial point is how to find a noise mask  $\epsilon$  that can effectively shift the embedding of a face away from its original counterpart and be visually non-intrusive. It is necessary to keep the noise mask as small as possible: placing a black oval on top of a face can surely cloak it, but the resulting face would also be unrecognizable by any human being. Previous works [19] solve this with a minimization problem, in which a dissimilarity metric, the DSSIM score [20], is used to measure how dissimilar two images are. Creating a noise mask  $\epsilon$ , or cloak then becomes a minimization problem of finding a value of  $\epsilon$  that can make a face be mistakenly classified and keep the DSSIM to a minimum.

We take a different approach, using thoroughly verified adversarial machine learning methods, namely the *Iterative Fast Gradient Sign* [17] (I-FGSM, in Eq. 4) and the *Iterative Least Likely Class* methods (in Eq. 5), to generate the noise masks, or cloaks, to apply on faces.

$$I'_0 = I, \quad I'_n = I'_{n-1} + \alpha * \text{sign}(\nabla_I J(\theta, I, y)) \quad (4)$$

$$\begin{aligned} I'_0 &= I, \quad y_t = \text{argmin}_y(p(y|I)) \\ I'_n &= I'_{n-1} - \alpha * \text{sign}(\nabla_I J(\theta, I'_{n-1}, y_t)) \end{aligned} \quad (5)$$

These methods, however, are designed around the loss functions of regression and classification models, such as *Cross Entropy* and *Mean Square Error*. In order to adapt them to the cost function  $J$  used in facial recognition neural networks, it is first needed to define all the components that play a role in the system. We use FaceNet as the network to perform our attacks on, and this uses the *Triplet Loss* function, outlined in Eq. 2. Because the network is already trained and we need a noise mask specific to a single face image, instead of computing the gradient of the cost function, we compute that of the loss function for a particular triplet of images. Triplet loss gives a measure of how close the anchor is to the positive and negative example. By inverting the positive with the negative example, the triplet loss shows how similar (or close) the anchor is to the negative example, and how far it is to the positive one. Its gradient is calculated with respect to the input to the network, so the pixel values of a face image tells how the input should be "updated" in order to make its embedding farther away from the positive example and closer to the negative one.

Noise masks are therefore defined as gradients of the triplet loss function relative to the inputs of the network, the pixel values making up face images. The cloaking problem is, therefore, reduced to a choice of positive and negative examples to use in the computation of gradients.

#### B. Components

##### Termination Condition

The hypothesis that "altering a face image so that its embedding is pushed far away from that of its original counterpart results in cloaking for that face image" holds true when an identifier has only one sample from the same person to compare a face against. Practically speaking, if person  $p$  has only one face image  $f_1$  in a labeled database, then if a new image  $f_N$  of the same person is altered with a noise mask  $\epsilon$  so that  $\|G(f_1) - G(f_N + \epsilon)\| > m$  and the margin  $m$  is large enough, then there is no way to associate  $f_1$  with  $f_N$  and  $f_N$  is said to be cloaked.

If there are multiple images in a database belonging to the same person that is trying to cloak a new face image  $f_N$ , say  $f_1$  and  $f_2$ , the situation is more complicated. Applying a noise mask on  $f_N$  to make it dissimilar to  $f_1$  may not have the same effect on the distance from  $f_N$  to  $f_2$ . One could argue that first applying a noise mask on  $f_N$  to make it dissimilar from  $f_1$ , resulting in  $f'_N$ , and then repeating the same process on  $f'_N$  to make it dissimilar from  $f_2$ , resulting in  $f''_N$ , may work, but this is not true. The second noise mask, in fact, could bring the newly generated face image  $f''_N$  closer to  $f_1$ , thus nullifying the effects of the first noise mask.

It is, therefore, necessary to not let the cloaking algorithm fall in a loop of generating noise masks effective for a data sample but not for another. This is solved by picking a halt condition independent from the data samples (anchor, positive and negative examples) being used. The algorithm generates noise masks  $\epsilon$  as long as the loss function returns positive values, and at each step, the embedding of the face being

cloaked moves significantly farther away from its original counterpart. This translates in a halt condition that stops the execution of the algorithm as soon as the loss  $L$  is 0 or the new distance is not meaningfully better than the previous, in other words, the difference in the distance with the previous iteration,  $\Delta d$ , is less than a threshold  $t$ . This makes it possible for the algorithm to certainly come to a halt.

The original *FaceNet* paper argues that two faces are said to belong to different people when their distance is greater than 1.242. This translates as a need to define a minimum distance that must be present between a cloaked image and its original version. Doing so assures that, at least during verification, the two images would be said to have different identities. This is achieved by tuning the margin used in the triplet loss function, which defines how different two distances must be to consider a triplet to be good (see Eq. 2).

Picking a large margin will push a face image very far away from its original counterpart's embedding, which may not always be possible. The maximum distance between two embeddings is limited by the mathematical conditions imposed by the hyperspace being used and the constraints on the embeddings. For *FaceNet*, faces' embeddings are designed to allow for a maximum distance of 4 units, and only for extreme cases. In our experiments, we registered maximum distances around 1.8, which means that it may not be possible to push an embedding farther away from another much more than that, considering the high dimensionality of the feature space and the requirement for noise masks to be minimal. Consequently, all experiments carried out in this research use margin values between 0.2 and 2. Varying this value has an effect on the intensity of noise masks introduced.

### Example Selection

FaceNet is a DNN trained to extract features from individual face images. During training, however, the loss function used is defined on three distinct images and, because our algorithm exploits backpropagation applied from the output of the loss function to the inputs of the network, all iterations of the proposed algorithm will require three images (an anchor, a positive example, and a negative example).

A positive example of a face image is simply another face image that portrays the same person. The negative is a face image of a different person. Telling whether two images represent the same person or not requires samples to be labeled. Alternatively, instead of picking positive and negative samples based on labels, they can be picked based on their embeddings' distances.

In our experiments, at the first iteration the positive example is always equal to the anchor. This significantly eases the example selection process and increases consistency among experiments. Deciding a positive example in any other way would not be meaningful: the closest example from a dataset may or may not belong to the same person, so it would introduce heavy inconsistencies in the experiments. This method does not impact the model negatively: starting from the second iteration, the anchor is different from the positive example (because of the cloak added). As for the negative example

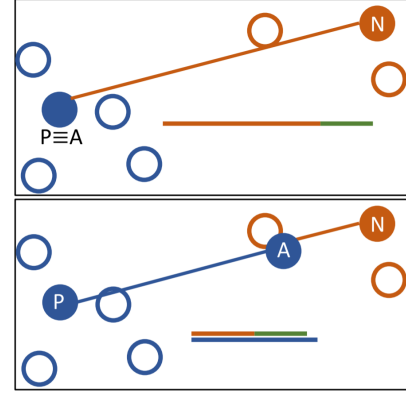


Fig. 1. Low dimensional representation of how embeddings are moved across the feature space. In the image above the distance to the negative example (in orange) plus the margin (in green) is greater than that to the positive example (in blue, which is 0), thus the loss, calculated switching the positive and negative examples, is  $> 0$ . When the anchor is close enough to the negative example, as in the picture below, the loss becomes 0

selection, we propose five different options, as explained in the following section.

### C. Dataset

We use FaceNet to carry out our experiments, loading its network structure and weights on startup without pre-compiling, allowing us to have access to the cost function of the model. The network we use is already trained, so we had no need to perform any further training.

We split our data into three subsets. The first subset is used for training only, and since the network we use is already trained, we will not consider it. The development dataset is usually used to quickly assess the performance of a neural network when this has not yet reached a final state. In other words, when testing different structures and parameters for a network, the development set is used for comparing how each performs.

The dataset used for development purposes is a subset of FaceScrub [21], originally composed of over 100,000 face images of 530 people. From this large database of images, 25 identities have been selected, and for each identity, ten images were taken, thus forming a set of 250 images. A dataset of this size would be too small for training, but it is sufficient for this case as it is only used to compare the performance of the algorithm when adjusting its parameters. All images in the development dataset (and later in the evaluation datasets) have been pre-processed by applying a close crop on the face and resizing the result to 96x96 pixels.

## IV. EXPLORATORY EXPERIMENTS

Face images are represented as matrices of size 3x96x96, which is also the shape of the gradients calculated with respect to the inputs. Given a gradient, we create a noise mask by normalizing its matrix so that the largest (or smallest) value is equal to  $\pm 2.5$ , thus capping the alteration of a pixel to 3% of its RGB value.

### A. Data

We evaluate the raw efficacy of each algorithm with a certain margin through the verification task. The dataset used for development is made of 250 images of 25 individuals, 10 per person, arranged in order of person but not labeled. Verification is, therefore, the task of verifying that all pairs of faces in the dataset with the same identity have similar embeddings, and those with different identities have dissimilar embeddings. For each face in the dataset, there are 9 other faces with the same identity, and 240 faces with different identities. Consequently, the dataset provides  $9 \times 250 = 2,250$  matching pairs and  $240 \times 250 = 60,000$  mismatching pairs of images. We look at both lists of pairs and calculate the *True Positive* and *False Positive* rates for 2,250 and 60,000 pairs, respectively. This is used as a raw efficacy measure to compare the performance of algorithms varying the margin and the negative example selection used.

We measure visual impact on the images using the *Structural Dissimilarity* (DSSIM) [20] between pairs of original and cloaked images. Each of the 250 sample images used is compared against their cloaked counterparts to calculate the DSSIM score. All DSSIM results for each experiment are saved to analyze them in terms of average, maximum, and standard deviation across experiments.

### B. Method 1 - Farthest Sample

The farthest face embedding is the one which should theoretically be most dissimilar to the face which is being cloaked, and intuitively is the most appealing choice. This will move the target image to the farthest class from it in the embedding space. This method is similar to what is used in the recently published Fawkes system [19], and it is an adaptation of the *Least Likely Class* method proposed in [14].

#### Algorithm

This first algorithm is among the simplest. The face whose embedding is farthest from that of the image being cloaked is picked as a negative example  $n$ . A single triplet is therefore formed using the face to cloak as both anchor and positive example, and the selected embedding's face as a negative example. Note that within the context of this research, the positive and negative examples are exchanged in place, so that the loss function's gradient indicates how to move the anchor towards the negative example.

Given the formed triplet, the cloaking algorithm iterates until either the loss function returns 0 or the embedding is moving towards the negative example too slowly. Fig. 1 shows a lower-dimensional example of this process, in which the negative example  $N$  is chosen as the farthest point from  $A$  (initially  $A \equiv P$ ). The loss function then returns the difference between the distance of the anchor to the negative example and to the positive example, in addition to the margin, or 0 if said value is negative. A loss greater than 0 indicates that the anchor is not closer to the negative example by at least the specified margin than it is to the positive example, so the face can still be altered to move it closer to the negative example. When the loss is positive, the situation is ideally that of Fig.



Fig. 2. Visual representation of how the margin value (in green) affects how far away a face image is pushed from its original version (in blue) towards the negative example (whose distance is in orange).

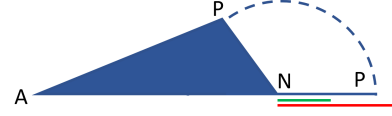


Fig. 3. Distance requirement between positive and negative example relative to the margin. If the margin is small, such as that in green, then  $\overline{NP}$  can be small. If it is larger though, such as that in red,  $\overline{NP}$  must be larger than it or the loss cannot converge to 0.

1 (a), and the cloaking algorithm iterates until the situation becomes that of Fig. 1 (b).

It is now easier to picture how changing the margin in the loss function affects the cloaking of images. When the margin is small, such as in Fig. 2 (a), a face needs to be only slightly closer to the negative example than to the positive example for the algorithm to stop. On the other hand, when the margin is larger, a face image is pushed much farther away from its original embedding (the positive example) and closer to the negative example (Fig. 2 (b)).

If the algorithm stops because the loss has become 0, the face image can be said to be cloaked completely (always within the extent forced with the margin). It is possible, however, that the margin is set too large for a particular image. Given a triangle formed with vertices  $P$ ,  $A$ , and  $N$ , as in Fig. 3, the triplet loss function would return 0 once the equation  $\overline{AN} + m < \overline{AP}$  is satisfied. This is possible only if  $\overline{NP} > m$ , which means that if the distance between the negative and positive examples is less than the margin  $m$ , the loss function never returns 0, and the algorithm iterates indefinitely. This is why if the delta of the distance between the anchor and the negative example between subsequent iterations is less than a threshold, the algorithm is halted. Such a threshold is common to all attack scenarios, and it is set at 0.01.

#### Performance

Using only a single triplet comes with some performance advantages. The main one comes from the initial choice of examples: looking for a single farthest sample, executed on a processor that supports vector operations, is a fast operation. On a low-powered laptop with a processor that supports AVX2 instructions it takes on average 2s to process a face image. In addition, since a single farthest example needs to be selected and a dataset only with a few hundred samples likely has gone far enough, the dataset used can be small. This second advantage, though, is quite minimal: our development dataset of 250 aligned face images takes up as less than 1.5MB of memory, so expanding or shrinking it would not bring any significant advantage.

We ran the cloaking algorithm on each of the 250 samples in our dataset. On average, noise masks show a cumulative alteration of about 45,000 pixel values per image or 1.6 units





Fig. 4. Effects of cloaking as described in algorithm 1.

per color per pixel (on a  $[0, 255]$  range). Such alteration is minimal, as a difference of 1.6 units per channel on each pixel is almost unnoticeable by the human eye. Fig. 4 shows how a face looks before and after being cloaked, both in its extracted, aligned form, and in its original shape within a larger image.

In terms of *Structural Dissimilarity* (DSSIM), the average value registered across all margins is 0.01. This is significantly lower than what is noticeable with a naked eye (0.2), so on average, the alteration is minimal and unnoticeable. The maximum DSSIM registered across all experiments with varying margin values is also well below the noticeable threshold, sitting at 0.035. As the margin increases, so does the DSSIM, and its values become more spread out too. At margin 0.2, the DSSIM has an average value of 0.0069 and a standard deviation of 0.0031, both gradually increasing until 0.0143 and 0.0061, respectively, when the margin is 2.0. On average, across all margin values, the registered DSSIM is 0.0104.

### Efficacy

The efficacy of this cloaking strategy is measured through verification comparing all possible pairs of images. Results show that the *True Positive* rate, which indicates what ratio of matching pairs are correctly verified is around 0.4 for all margins used, from 0.2 to 2.0 (equivalent to the 40% of pairs). For comparison, the *True Positive* rate for the original, uncloaked 250 samples is 0.91. Cloaked images are, therefore, on average, across margin values, over 50% less likely to be correctly identified.

Opposite to the reduction in *True Positive* rate is an increase of the *False Positive* rate, which measures how many mismatching pairs are wrongly labeled as matching. The original, uncloaked images yield a 0.06 rate, which translated to 6% of mismatching pairs to be labeled matching, and this number increases to 0.08 0.11 when images are cloaked. In relative terms, 33% to 83% more pairs of faces are mistakenly labeled.

What is surprising is that as the margin grows larger (and, as shown previously, the DSSIM score increases), the *True Positive* rate actually increases. This is as if forcing faces' embeddings farther away from their original position in the feature hyperspace would somehow group them together again. An example of this in a lower-dimensional space is given in Fig. 5. In contrast with these figures, the *False Positive* rates also increase. Putting these two trends together, forcing a larger margin for the *Triplet Loss* function makes embeddings converge slightly in the same area, as both the *True Positive* and *False Positive* rates increase.

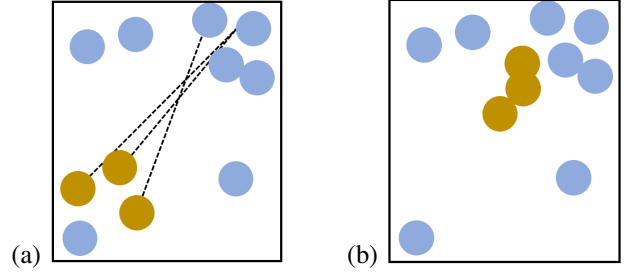


Fig. 5. Example of a failed cloaking attempt when selecting the most dissimilar data samples as the target: the embeddings of images of the same person (in yellow) have actually moved closer from (a) to (b), even if each in (b) is supposed to be anonymized.

### C. Method 2 - Random Samples

A potential issue with the previous strategy - using the farthest sample as a negative example for triplets - was given by the direction towards which embeddings were shifted. For a group of images belonging to the same person, and thus whose embeddings are similar too, it is likely that the negative examples picked for each are the same sample or samples nearby. The result is that embeddings are moved in the same direction, and in the worst case, they remain close to one another. At this point, performing clustering on such cloaked images would yield quite accurate results.

A possible solution to ensure that the embeddings of images are more scattered is to pick random examples. The main advantage over selecting the farthest sample is that the embeddings of faces of the same person are likely to be moved in different directions, thus making it more difficult to cluster them. A drawback is that, depending on which sample is picked, the noise mask applied on the face may not be sufficient for the latter to be misidentified. This is the case when the randomly selected embedding is very close to the embedding of the face to cloak.

#### Algorithm

To prevent selecting a negative example that is too close to the anchor, we select multiple random examples for a single face to try to cloak. Instead of forming a single triplet, multiple are created. For each triplet formed, the cloaking algorithm is executed as in the previous algorithm. Once the algorithm halts, the next triplet is selected, and the algorithm is restarted. This is done until all triplets have been processed. We use  $k = 5$  for the number of random negative examples to select from the dataset.

The noise masks applied on the faces are cumulative across cloaking iterations with each triplet. Once a face (or anchor) is cloaked relative to the first formed triplet, the resulting cloaked anchor is used in the next triplet. The positive example, or the original face's embedding, is kept fixed across all triplets: this ensures that no matter what negative example is chosen, the anchor will always move farther away from its original position, and never closer. For each new triplet processed, the number of steps required for the algorithm to stop is reduced. This is because being the positive example fixed, once the anchor is far enough from it, for subsequent triplets, the loss

may be already close to 0, thus requiring fewer iterations to come to a halt.

### Performance

Cloaking faces using multiple negative examples comes with a higher computational cost, though it is minimal. Because the cloaks applied on face images are cumulative, the effects carry over across triplets, and it becomes increasingly faster for the algorithm to come to a halt. The computational cost in terms of time required to process each face image has increased by around 50%, from 2s to 3s on the same low-spec machine.

The DSSIM scores have also increased compared to the previous algorithm. On average across all values of the margin, the DSSIM has increased by 0.0052 points to 0.0156, a 50% relative increase. Even if cloaked images are significantly more altered, the dissimilarity between them and their original counterparts remains well below the noticeable threshold (0.2).

### Efficacy

The verification accuracy in terms of *True Positive* rate for this algorithm is significantly lower than that of the previous, with values ranging from 0.37 down to 0.21: this corresponds to a 59% to 77% decrease in verification accuracy. The verification accuracy when images are cloaked following this algorithm drops from 91% to 37.21%. This shows that selecting multiple random targets to cloak a face is more effective than selecting a single farthest one.

The *False Positive* rate for this strategy, on the other hand, oscillates between 0.07 and 0.09, for a relative efficacy of up to 50% (as up to 3% more samples are mistakenly considered matching). The *False Positive* rates higher (and therefore yielding more misclassifications) are worse than in the previous strategy. This said, the *True Positive* rate, which matters most for facial identification, is decreased more significantly, and therefore this is a superior strategy.

### D. Method 3 - Random & Farthest Samples

Selecting multiple random negative examples proved to be a better overall strategy than picking a single, farthest example. However, the *Least Likely Class* method requires that the "least likely" class (in this case, the farthest example) is to be picked for best performance. We, therefore, propose a union of the previous two algorithms in an attempt to mitigate the drawbacks of each, namely the relatively poor performance of the first and the potential unpredictability of the second (when 5 random negative examples are chosen, the probability that they all belong to the same person as the anchor is as low as  $10^{-9}$  using our development dataset, but said targets are nonetheless not guaranteed to be much dissimilar from the anchor).

### Algorithm

The algorithm that implements this algorithm is almost the same as the previous one. The only difference is that an additional sixth triplet is used, and this uses the farthest sample from the dataset as a negative example. This triplet is processed first, then the ones containing random examples are processed similarly.

The core idea behind this combined strategy is to introduce a small amount of noise to the images being cloaked so that the embeddings of a single person's images do not risk being pulled around the same target, as in Fig. 5. This strategy should, therefore, hinder clustering the data points and further decrease the true positive verification rate.

### Performance

The time required to process each image is, on average equal to that of the previous algorithm, which was using 5 instead of 6 triplets. The DSSIM scores also remain equal to those of the previous strategy, sitting at 0.0157 on average. The combined usage of the farthest sample and some random ones, therefore, comes at the cost of having both a higher computational toll and a heavier visual impact on the images (while still being only a fraction of the visually noticeable threshold).

### Efficacy

Surprisingly, this strategy yields worse changes in the *True Positive* rate for the verification task. If looking at the farthest example alone made the rate of correctly identified matches drop to 0.40, and using 5, random examples had an average rate of 0.29, using both gives 0.44. Specifically, the *True Positive* rate ranges from 0.37 and 0.52: the best performing values for the margin in this strategy give results no better than those of the worst-performing values using random targets only.

The *False Positive* rate ranges from 0.08 and 0.095, with average at 0.085. This is not significantly better than any previous strategy. Considering both the performance and the efficacy outcomes of this algorithm, this can be considered the worst of the ones considered so far.

### E. Method 4 - Most Similar Sample

Performing experiments using a strategy that logically seemed to be best that others actually yielded the worst results. We, therefore, propose a fourth way to select the negative target examples to perform targeted cloaking, even if, at first glance, the selection is not optimal. So far, targets have been selected based on how far they were and introducing randomization to increase the chances that images' embeddings of the same people would be cloaked away from one another. A new proposal for targets is to pick those which are most similar to the images being cloaked.

### Algorithm

Instead of using the most dissimilar or farthest away embeddings as target(s), this algorithm uses the most similar examples from the dataset. As explained in section IV-B, in order for the *Triplet Loss* function to return non-zero values (and therefore for the generation of noise masks to succeed), the distance between the negative example and the anchor must be greater than the sum of the margin and the distance between the positive example and the anchor. As the positive example is set equal to the anchor in the first iteration, such constraint can be rewritten as the distance between the positive and the negative example must be greater than the margin. Such is the condition for the gradient of the loss function to be non-zero.

The negative example is therefore chosen as the most similar sample by picking the closest sample to the anchor (the face to cloak) which is also distant from the anchor by at least the margin  $m$ . The formula for such selection of target  $y_t$  given a face image (anchor)  $I_a$  and a dataset of embeddings  $E$  is then:

$$y_t = \arg \min_i (\|G_W(I_a) - E'_i\|) \quad (6)$$

$$E' = \{e \mid e \in E \wedge \|G_W(I_a) - e\| < m\}$$

### Performance

Using the most similar (and yet far enough) sample from the dataset yields similar or better performances compared to previous strategies. As far as computational time goes, the time required to process images decreases slightly to an average of 1.7s per sample, a shy 15% decrease from the first algorithm's.

What shows a more significant improvement, on the other hand, is the DSSIM achieved in this algorithm. It is 0.0074 on average, showing a 29% reduction when compared with the best average score achieved so far, 0.0103 from the first algorithm. The maximum value registered is 0.0346, which is acceptable by a large margin.

These results are not particularly surprising, as cloaking a face image using a similar image as the target would logically produce less visible noise masks. As per the processing speed of samples, this is also expected to increase as the loss function reaches 0 faster when the positive and negative examples are closer to each other.

### Efficacy

What is instead an unexpected result is the efficacy of this algorithm. The *True Positive* rates vary greatly depending on the margin used, from 0.87 at margin 0.2 (which is an insignificant accuracy reduction) down to 0.08 as the margin approaches 2.0. As the margin increases, in fact, the *True Positive* rate decreases to results that not even a random target selection could achieve. In relative terms, the accuracy drops by up to 91% compared to the verification of pairs of original images. This is, by far, the best result.

The *False Positive* rate for this strategy is also largely dependent on the value of the margin. To give a few examples, the rate is 0.07 at margin 0.2, then decreases slightly to 0.06 until margin 0.6, and increases until a maximum of 0.11 at margin 1.4. Such results are significantly oscillating, and yet never lower than those obtained using the original images; instead, the *False Positive* rates increase up to 83%.

### F. Method 5 - No Sample Selection

The best algorithm analyzed so far is also the one expected to perform the worst. We, therefore, push the idea of selecting a similar sample for the negative example to its extreme by choosing the anchor itself. While at first, it may seem counter-intuitive to cloak an image using as target the image itself, we hypothesize that the gradient so calculated corresponds to the gradient as calculated following the *Fast Gradient Sign Method* [14].

The difference between the *Fast Gradient Sign* and the *Least Likely Class* methods is the usage or not of a target to direct

the change in the input data. When a target is used, the gradient of the loss function indicates how to alter the input to make it more similar to the target or how to minimize the loss in relation to the target; on the other hand, if a target is not used, the gradient is used to maximize the loss as calculated with the true class. The latter case can be translated in the context of feature extractors as maximizing the representational inaccuracy of a data sample. This description can be further tuned to the context of a facial recognition neural network that generates embeddings as cloaking a face to make its embedding as inaccurate as possible.

### Algorithm

Simply enough, this algorithm requires the anchor to be selected as both the positive and the negative example at the first iteration. Starting from the second iteration of the algorithm, as the anchor will have one noise mask applied already, the anchor will be different from both the examples forming the triplet.

What is interesting about this strategy is that the loss function returns a constant value, as the distance between the anchor and the negative example is always equal to that between the anchor and the positive example.

As the margin changes, however, the noise masks generated are always the same. As detailed in section IV, the gradient calculated from the loss function relative to the input layer is normalized so that the maximum (or minimum) value is always  $\pm 2.5$ . Consequently, to this constraint, no matter what margin value is used, the cloaks generated with this strategy are always the same, as proven by all results.

### Performance

Cloaking face images using a single triplet was always comparatively fast in previous experiments, but it was so because as soon as the loss function returned a value of 0 the algorithm would stop (which was the halt condition being triggered in most cases). As the value of the loss function is constant in this case, the halt condition is reduced to checking the delta of the distance across iterations until it falls below the threshold. Consequently, the time required to process each image is increased to around 3s, closely relating to the processing time registered when using multiple random negative examples.

As for the intensity of the alterations introduced in the image, this is kept low. The average DSSIM score is 0.0099, about 4% lower than that using the farthest sample as a negative example, with a maximum of 0.0332 - also slightly lower than that of the first algorithm.

### Efficacy

The most interesting result of this algorithm is the *True Positive* rate when verifying pairs of images with matching identities: 0.084, which means only 8.4% of the pairs are correctly verified. This is a hindering of 90% of the accuracy of verification for cloaked face images, the best result among all algorithms.

Despite the *True Positive* rate being very low, the *False Positive* rate is low, too, even more than that of uncloaked images: 0.027. A rational explanation to this event is that the embeddings of the faces are altered in a manner that scatters



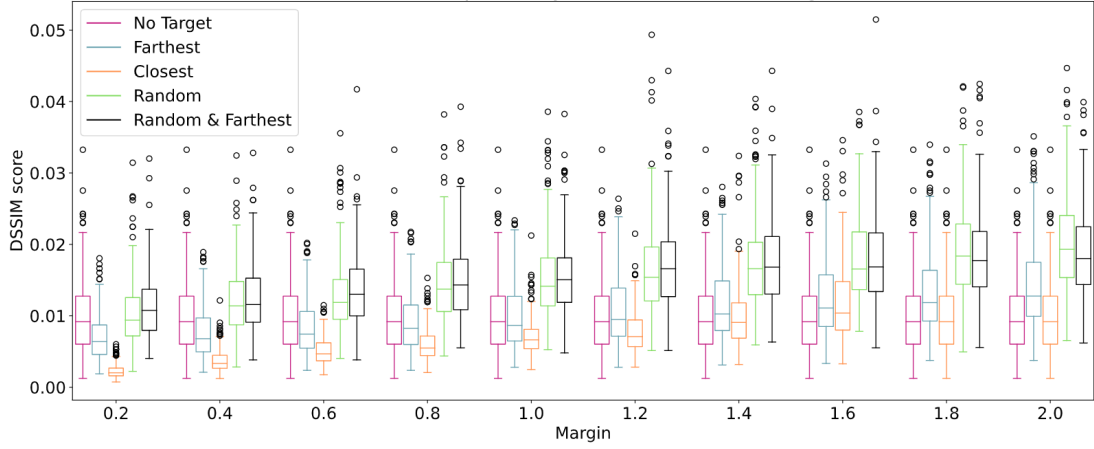


Fig. 6. DSSIM values registered in each experiment for the five algorithms proposed.

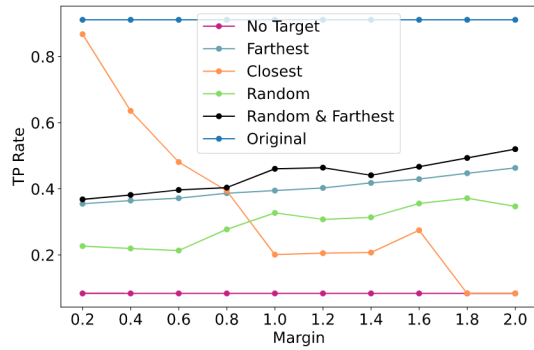


Fig. 7. True Positive rates for each experiment (and including for the original faces' embeddings).

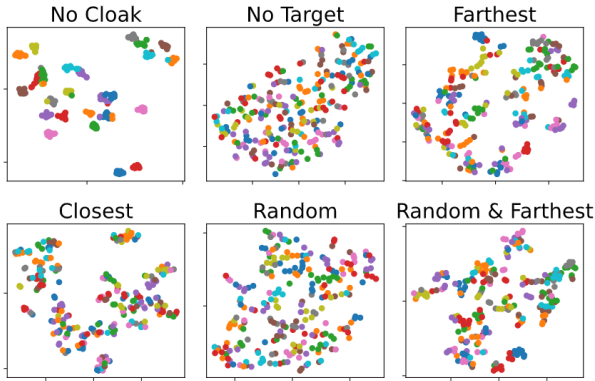


Fig. 8. Visualization on a 2D plane of the embeddings using t-SNE. The embeddings are cloaked using a margin of 1.0 (where applicable).

them far away from one another on subsets of features for which uncloaked faces' embeddings have a small variance.

### G. Results Summary

Of the five cloaking strategies analyzed to promote cloaking of face images, selecting the same positive and negative examples was the optimal strategy. While each strategy's outcomes were described in detail and included informative

comparisons, a visual overview of the results can better help understanding how strategies compare to one another.

The first comparative analysis proposed is that of the DSSIM scores registered. For each of the five algorithms and each of the 10 values proposed for the margin, a visual analysis of the DSSIM of pairs of images before and after being cloaked is shown in Fig. 6. The boxplots help visualize all the statistics of important for a strategy, and particularly the average and maximum values, which are key in assessing the usability of a cloaking strategy. Note that the *Most Similar* algorithm's results go as far as having a margin of .16. This is because, for larger margins, there may be no pairs of images to select for positive and negative examples as described in Eq. 6. The graphs show a tendency towards higher values as the margin is increased, with the exception of the selection of no targets in the fifth algorithm, whose outcome is independent of the margin's value.

A second important graph to analyze is that of the *True Positive* rates in Fig. 7, which includes a data point per combination of algorithm and margin selected. As for the previous figure, the algorithm using the most similar sample as a negative example is plotted for margin values up to .16 only. The graph shows a general and slight increase in verification accuracy as the margin increases for algorithms based on cloaking images by selecting examples far away. In contrast, selecting nearby samples as targets yields better results as the margin is set to be larger.

A final visualization of the effects of cloaking images with different cloaking techniques is given by the graphs in Fig. 8. Each scatter plot shows the results of performing *T-distributed Stochastic Neighbor Embedding* (t-SNE) [22] on the embeddings. This is a non-linear technique to reduce high-dimensional vectors to a smaller subset of features. Similar to how *Principal Component Analysis* works, this technique yields the best results when processing data with a large number of features. The top-left graph shows how embeddings are simplified in two dimensions, with each point representing an embedding and being colored according to the identity of the person portrayed. Not surprisingly, the original face

images' embeddings form very distinct clusters. Once images are cloaked, however, their embeddings are more scattered around. It can be seen that the first algorithm proposed produces embeddings with still form clusters to some extent. Randomly picking 5 targets as negative examples produce more scattered results, while the best cloaking results are given by setting the negative and positive examples equal to one another: this latter case does not allow any clusters to be inferred.

## V. EVALUATION

This section proposes a complete evaluation of the effects of cloaking images with our system, and it does so for three different tasks: verification, identification, and clustering. For each of these task, we use an appropriate dataset. We test verification on the Labelled Faced in the Wild (LFW) [23] dataset, and test identification and clustering on the *FaceScrub* [21] and *PubFig83* [24] datasets. Following is a description of each of the tasks.

**Verification** is the task of checking if two images represent the same person or not. LFW provides 3000 pairs of images of the same people and 3000 of different people, and the accuracy of the verification task is calculated as the ratio between the number of pairs correctly labeled as "same person" and the ones available (*True Positives*), and the number of different people's pairs wrongly labeled as "same person" (*False Positives*) among those available. A real-world application of this can be the verification of an employee's identity given his ID card before entering a corporate building.

**Identification** is the task of, given a labeled dataset of faces, finding the label of new face images whose real identity is among those contained in the dataset. In real life, this could be the case when a user uploads a new image of himself or of friends on a social network, after having already uploaded some images of the same people in the past, and a third-party entity tries to match those new faces with ones it already has.

**Clustering**, is the task of trying to label a fairly large number of images with no prior knowledge of them. An actual application of this would be to separate a set of images in groups containing each the same person when no labeled images for those people are available.

Note how each subsequent task uses less information than the previous. Verification is a true or false problem which, given a large amount of data (two images), only tries to predict one bit of data. Identification, on the other hand, is a classification task, and the answer is more complex than just a yes or no: a class, or a label, is the result of the task, and there could be many labels to choose from. This said, identification is advantaged by the usage of a labeled dataset, and therefore it has a fairly large amount of information to start with. Finally, clustering is similar to identification in terms of required output, as it predicts an identity or label for each data point. In contrast with identification, however, it does not have a labeled dataset for reference; thus, it is the task that demands the least amount of information to achieve the same result.

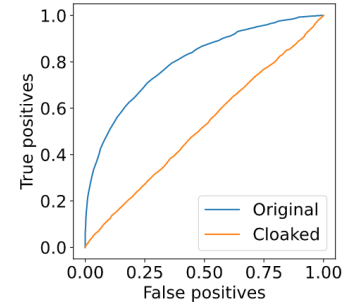


Fig. 9. Comparison of the verification performance on LFW between the original and the cloaked images.

We, therefore, assess the performance of our best performing algorithm for each of the levels of information that an entity doing identification may have: a single image for each person, on which only verification is to be done; multiple labeled images for each person; multiple, unlabelled images for each person.

### A. Verification

Verification is used to check whether two images represent the same person or not. It is a widely used evaluation metric for the representational accuracy of facial feature extractors, and we provide a complete study of the effectiveness of our algorithm for this task.

We use the LFW dataset with its lists of matching and mismatching pairs of images to assess the effects of the cloaks applied to images. Verification is done comparing two images' embeddings by computing their Euclidean distance and classifying them as a match if this distance is less than a threshold. Different thresholds yield different performances: a low threshold would give a very low error rate for *False Positives*, but also a low *True Positive* rate; setting it to a higher value should dramatically increase the *True Positive* rate, but at the cost of registering higher *False Positive* rates too.

Fig. 9 shows the ROC curve typically used to evaluate the performance of a facial feature extractor for the verification task. The graph is obtained by setting the threshold to 0 and increasing it with steps of 0.02 until it reaches the value of 3.0 (for a total of 150 values) and calculating the true and false-positive rates for the embeddings used. For comparison, two curves are plotted: the first is calculated using the embeddings as extracted from the original images, while the second is calculated on those of the cloaked images. While verification is not perfect on the original face images, it yields quite a high accuracy while keeping the *False Positive* rate to a minimum. When images are cloaked, however, verifying whether two images represent the same person or not is almost exactly as accurate as tossing a coin to decide. The cloaks applied to the images have, therefore, successfully made it impossible to extract information from them via verification alone.

## B. Identification

Facial identification is the task of labeling a face image with a label from a set of known identities, and therefore it requires a labeled initial dataset. This is an important case, because even if the user cloaks their images, prior uncloaked images may still exist or be uploaded by third parties. This task is harder to tackle than verification because there are many techniques available and having multiple images of the same person makes it easier to extract information and label faces.

This experiment is therefore used to evaluate the efficacy of our proposed cloaking algorithm against identification methods. Both cases described earlier are analyzed: when a labeled dataset is formed with uncloaked images (such as by running clustering on the faces' embeddings) and when it is formed with cloaked images (which requires manual labeling). We explore five different identification strategies, so to make sure results are assessed as thoroughly as possible. In this section, we use  $E$  to refer to the set of labeled embeddings and  $f$  for the function mapping the index of an embedding to its corresponding label.

For identification, we use the following algorithms:

- Nearest Neighbor
- Nearest Centroid
- K-Nearest Neighbors
- Weighted K-Nearest Neighbors
- Distance-Bound Nearest Neighbor

When we first explored identification on the FaceScrub and PubFig83 datasets, we found surprisingly bad results. For example, we started by setting aside 10 images for each person and building a labeled dataset with the remaining images. Then, identifying those 10 images per person not included in the labeled dataset gave accuracy scores around 5 ~ 10% for all five identification methods used. Such low scores using uncloaked images only were alarming, at first.

Diving deeper into the issue, we analyzed the relationship between the size of the labeled dataset used and the performance of identification. We found an interesting relationship between the two. Contrary to intuition, the larger the labeled dataset, the worse the performance of identification. This is true for both dimensions of the dataset: depth and breadth.

Before being able to effectively evaluate the effects of cloaking images in identification tasks, it was necessary to define an effective identification scheme that would work well on the original datasets. We have analyzed the performance of the previously described identification strategies with respect to the breadth and depth of the labeled dataset. For the breadth, which in this case corresponds to the number of people included in the dataset, we have chosen values ranging from 2 to 83, which is the number of people included in PubFig83. For depth, which is how many samples are labeled for each person, we have chosen values 5, 20 and 80.

The graphs in Fig. 10 show how the accuracy of identification, calculated as the number of correctly identified images over the number of images processed, with 1 being a perfect score. Each of the three graphs shows a different

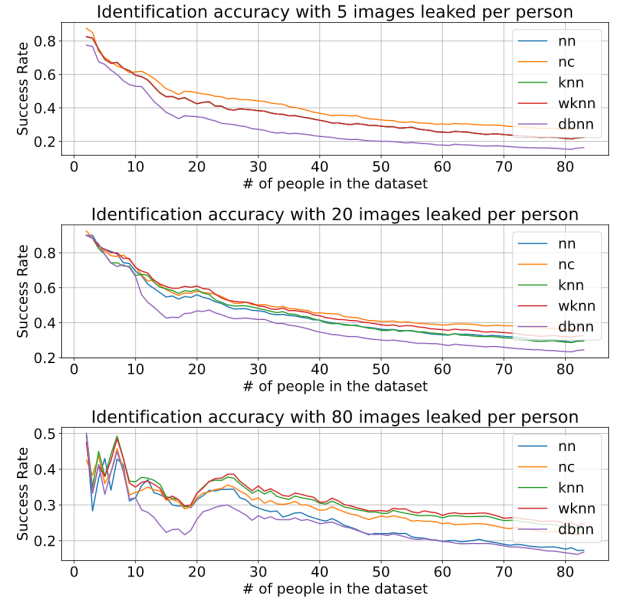


Fig. 10. Comparison of the accuracy of the five identification methods varying the depth and the breadth of the labeled dataset used.

value for the depth of the labeled dataset, while the breadth of said dataset is varied on the abscissas. Depths of 5 and 20 samples per person show comparatively good results, while the performance drops when the parameter is raised to 80. This shows how using a deeper dataset not only does not improve identification accuracy, but instead hinders it. The same applies to the breadth of the dataset. An initial thought was that this phenomenon was caused by overfilling the feature space with embeddings, so many that the boundaries between clusters of the images of the same people were not clear anymore. A closer look at the numbers shows that identification actually performs increasingly better as the size of the dataset grows than assigning labels at random. Fig. 11 illustrates how many times better is each identification method over assigning labels at random, which is the baseline score. The data is obtained by averaging the accuracy scores over the three depth configurations for datasets with a breadth from 2 to 83 people. When 5 people's images are included in the labeled dataset, the performance of identification is threefold that of randomly assigning labels, and becomes tenfold when 26 people's images are used. While the relative performance gain grows with the dataset size, the absolute accuracy of identification still decreases, and it is thus not advised to use large datasets.

We evaluate identification as a hundredfold average of the accuracy obtained by building a labeled dataset with 20 images per each of 20 people at random from those available. We do this for both the FaceScrub and the PubFig83 datasets. We compare how uncloaked images are classified when uncloaked images are included in the labeled dataset. The same is then done trying to identify cloaked images. Finally, cloaked images are used both in the labeled dataset and as those to be identified. These three settings correspond to a base case where

	PubFig83			FaceScrub		
	All clear images	Clear images in dataset only	All cloaked images	All clear images	Clear images in dataset only	All cloaked images
Nearest Neighbor	20.08%	6.73% (-66.46%)	7.00% (-65.15%)	59.02%	11.20% (-81.03%)	8.47% (-85.66%)
Nearest Centroid	25.45%	8.12% (-68.08%)	7.93% (-68.84%)	57.88%	11.28% (-80.52%)	8.43% (-85.45%)
k-NN	21.27%	7.04% (-66.88%)	6.47% (-69.56%)	57.37%	11.22% (-80.45%)	7.93% (-86.18%)
Weighted k-NN	22.77%	7.13% (-68.67%)	6.65% (-70.78%)	60.98%	11.57% (-81.03%)	8.72% (-85.71%)
Distance-bound NN	14.53%	7.40% (-49.07%)	7.32% (-49.59%)	14.18%	09.83% (-30.68%)	8.14% (-42.60%)
Mean	20.82%	7.29% (-63.83%)	7.08% (-64.78%)	49.89%	11.02% (-70.74%)	8.34% (-77.12%)

TABLE I  
IDENTIFICATION ACCURACY SCORES FOR THE FIVE METHODS PROPOSED.

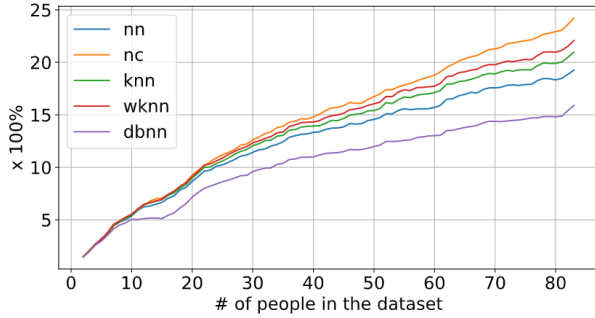


Fig. 11. The relative performance gain of identification over randomly assigning labels.

identification is done on normal images, a leak scenario in which an identifier has a labeled dataset of clear images, but the images to the label are cloaked, and the last scenario in which all images are cloaked and the labeled dataset must have been built manually.

The task is to identify 10 faces for each of the 20 people in the dataset splits. This experimental setup is similar to a real-world application of facial recognition to identify individuals from a small pool of known people. For example, this is the case of a social network labelling faces from a user's uploaded image using a labelled dataset formed with images of said user's close friends. The results, shown in table I, show that cloaked images reduce the accuracy of identification by over 50% using both FaceScrub and PubFig83. What is most interesting is that whether or not clear images are leaked, new cloaked images are still difficult to identify. Given that random assignment of a label when 20 labels are available yields 5% accuracy on average, accuracy scores around 7 ~ 11% are only marginally better than randomly guessing.

### C. Clustering

The final evaluation for the effectiveness of our cloaking system is done via clustering. The goal is to look at whether it is possible, in an unsupervised manner, to group together face images of the same individuals. As done previously, we first look at how well clustering works when performed on the original, unaltered face images. We compare this to when 10% of the images, picked at random, are cloaked, then when 50% are, and finally when only cloaked images are used.

	PubFig83		FaceScrub	
	Config 1	Config 2	Config 1	Config 2
0% cloaked	27.18%	22.95%	48.07%	42.52%
10% cloaked	25.57% (-5.92%)	20.62% (-10.15%)	43.86% (-8.76%)	36.15% (-14.98%)
50% cloaked	21.79% (-19.83%)	17.30% (-24.62%)	30.25% (-37.07%)	22.59% (-46.87%)
100% cloaked	18.03% (-33.66%)	15.47% (-32.59%)	20.36% (-57.65%)	16.50% (-61.19%)

TABLE II  
CLUSTERING ACCURACY SCORES ON TWO DATASETS, PUBFIG83 AND FACESCRUB, AS DIFFERENT RATIOS OF IMAGES ARE CLOAKED. THE FIRST CONFIGURATION 'CONFIG 1' REFERS TO CLUSTERING WITH  $d = 1.242$  STOP CONDITION, THE SECOND WITH A STOP CONDITION DEPENDENT ON THE NUMBER OF CLUSTERS FORMED (20).

Measurements are also results of a hundredfold average for datasets with 20 people having each 20 images.

The clustering accuracy of a method is calculated by looking at the individual clusters. For each cluster, its most frequent item is taken as the cluster identifier; then, the percentage of images in the cluster belonging to the same person is calculated, and a weighted average is made among all clusters identified (excluding clusters with a single item). This measurement allows a single person's images to be split into two clusters but still yield a 100% accuracy if both clusters only include images of that person and are not outliers, thus allowing large differences in a person's look across images (e.g., haircuts and aging effects) to not negatively affect the score.

This evaluation is performed using agglomerative clustering with two stop conditions: either when the target number of clusters is reached (20), or when subsequent agglomerations exceed a maximum distance threshold of 1.242 (which allows the formation of multiple clusters per each person). As a consequence, the table II reports two measurements for each experiment, one per stop condition of the clustering algorithm. The resulting accuracy scores, though already fairly low using uncloaked images only, show a significant decrease as the percentage of cloaked images increases. When all images are cloaked, compared with when they are not, faces are over 30% less likely to be correctly clustered as measured on PubFig83 and over 50% when FaceScrub is used.

## VI. CONCLUSION & FUTURE WORK

Of the five target selection strategies proposed, the most effective strategy was selecting any target at all. This makes sense in the context of feature extraction. Neural network classifiers are more vulnerable to attacks that make them mislabel a sample for another particular sample, thus focusing on introducing disturbances in images towards a specific output class. Feature extractors, on the other hand, do not have any pre-defined output classes, and this research shows that non-target strategies, rather than directing an adversarial attack towards a particular target yields optimal results.

The algorithms proposed are executed in a *white-box* environment, which may not always be accessible. When a facial recognition neural network is inaccessible it becomes impossible to compute the gradients of the cost function, and attacks cannot be executed. The transferability of adversarial examples is an emerging field of adversarial machine learning that examines how *black-box* attacks can be executed in *white-box* settings. However, no studies on its application in feature extractor facial recognition models currently exist. Recent research proved that transferability works to a certain degree for facial recognition classifiers, so it may also be applied to feature extractors in the future.

A second note must be made on the training of the neural network being used. Neural networks are often trained with the insertion of adversarial examples too, with the goal to mitigate the negative effects that crafted examples can have on a model once it is trained. We do not know whether it is possible or not to strengthen facial recognition neural networks by including some adversarial examples generated with our algorithms, but we feel this would be an interesting area for future work.

## REFERENCES

- [1] European Parliament and Council of European Union, "Regulation (eu) 2016/679," 2016, <http://data.europa.eu/eli/reg/2016/679/oj>.
- [2] "Are Organizations Ready for New Privacy Regulations?" [Online]. Available: <https://www.internetsociety.org/resources/ota/2019/are-organizations-ready-for-new-privacy-regulations/>
- [3] J. P. Pesce, D. L. Casas, G. Rauber, and V. Almeida, "Privacy attacks in social media using photo tagging networks: a case study with Facebook," in *Proceedings of the 1st Workshop on Privacy and Security in Online Social Media - PSOSM '12*. Lyon, France: ACM Press, 2012, pp. 1–8. [Online]. Available: <http://dl.acm.org/citation.cfm?doid=2185354.2185358>
- [4] J. Bromley, J. W. Bentz, L. Bottou, I. Guyon, Y. Lecun, C. Moore, E. Säckinger, and R. Shah, "Signature verification using a "siamese" time delay neural network," *International Journal of Pattern Recognition and Artificial Intelligence*, vol. 07, no. 04, pp. 669–688, Aug. 1993. [Online]. Available: <https://www.worldscientific.com/doi/abs/10.1142/S0218001493000339>
- [5] S. Chopra, R. Hadsell, and Y. LeCun, "Learning a Similarity Metric Discriminatively, with Application to Face Verification," in *2005 IEEE Computer Society Conference on Computer Vision and Pattern Recognition (CVPR'05)*, vol. 1. San Diego, CA, USA: IEEE, 2005, pp. 539–546. [Online]. Available: <http://ieeexplore.ieee.org/document/1467314/>
- [6] F. Schroff, D. Kalenichenko, and J. Philbin, "FaceNet: A unified embedding for face recognition and clustering," in *2015 IEEE Conference on Computer Vision and Pattern Recognition (CVPR)*. Boston, MA, USA: IEEE, Jun. 2015, pp. 815–823. [Online]. Available: <http://ieeexplore.ieee.org/document/7298682/>
- [7] Y. Taigman, M. Yang, M. Ranzato, and L. Wolf, "DeepFace: Closing the Gap to Human-Level Performance in Face Verification," in *2014 IEEE Conference on Computer Vision and Pattern Recognition*. Columbus, OH, USA: IEEE, Jun. 2014, pp. 1701–1708. [Online]. Available: <http://ieeexplore.ieee.org/lpdocs/epic03/wrapper.htm?arnumber=6909616>
- [8] —, "Web-scale training for face identification," in *2015 IEEE Conference on Computer Vision and Pattern Recognition (CVPR)*. Boston, MA, USA: IEEE, Jun. 2015, pp. 2746–2754. [Online]. Available: <http://ieeexplore.ieee.org/document/7298891/>
- [9] Y. Sun, Y. Chen, X. Wang, and X. Tang, "Deep learning face representation by joint identification-verification," in *Advances in Neural Information Processing Systems* 27, Z. Ghahramani, M. Welling, C. Cortes, N. D. Lawrence, and K. Q. Weinberger, Eds. Curran Associates, Inc., 2014, pp. 1988–1996. [Online]. Available: <http://papers.nips.cc/paper/5416-deep-learning-face-representation-by-joint-identification-verification.pdf>
- [10] Y. Sun, X. Wang, and X. Tang, "Deep Learning Face Representation from Predicting 10,000 Classes," in *2014 IEEE Conference on Computer Vision and Pattern Recognition*. Columbus, OH, USA: IEEE, Jun. 2014, pp. 1891–1898. [Online]. Available: <http://ieeexplore.ieee.org/lpdocs/epic03/wrapper.htm?arnumber=6909640>
- [11] —, "Deeply learned face representations are sparse, selective, and robust," in *2015 IEEE Conference on Computer Vision and Pattern Recognition (CVPR)*. Boston, MA, USA: IEEE, Jun. 2015, pp. 2892–2900. [Online]. Available: <http://ieeexplore.ieee.org/document/7298907/>
- [12] Y. Sun, D. Liang, X. Wang, and X. Tang, "Deepid3: Face recognition with very deep neural networks," *arXiv preprint arXiv:1502.00873*, vol. abs/1502.00873, 2015.
- [13] L. Huang, A. D. Joseph, B. Nelson, B. I. Rubinstein, and J. D. Tygar, "Adversarial machine learning," in *Proceedings of the 4th ACM Workshop on Security and Artificial Intelligence*, ser. AISec '11. New York, NY, USA: Association for Computing Machinery, 2011, p. 43–58. [Online]. Available: <https://doi.org/10.1145/2046684.2046692>
- [14] I. J. Goodfellow, J. Shlens, and C. Szegedy, "Explaining and harnessing adversarial examples," 2014.
- [15] S.-M. Moosavi-Dezfooli, A. Fawzi, and P. Frossard, "DeepFool: A Simple and Accurate Method to Fool Deep Neural Networks," in *2016 IEEE Conference on Computer Vision and Pattern Recognition (CVPR)*. Las Vegas, NV, USA: IEEE, Jun. 2016, pp. 2574–2582. [Online]. Available: <http://ieeexplore.ieee.org/document/7780651/>
- [16] A. Kurakin, I. Goodfellow, and S. Bengio, "Adversarial machine learning at scale," 2016.
- [17] —, "Adversarial examples in the physical world," *ICLR Workshop*, 2017. [Online]. Available: <https://arxiv.org/abs/1607.02533>
- [18] R. Awasthi, "Breaking Deep Learning with Adversarial examples using Tensorflow," May 2018. [Online]. Available: <https://cv-tricks.com/how-to-breaking-deep-learning-with-adversarial-examples-using-tensorflow/>
- [19] S. Shan, E. Wenger, J. Zhang, H. Li, H. Zheng, and B. Y. Zhao, "Fawkes: Protecting privacy against unauthorized deep learning models," in *29th USENIX Security Symposium (USENIX Security 20)*. USENIX Association, Aug. 2020, pp. 1589–1604. [Online]. Available: <https://www.usenix.org/conference/usenixsecurity20/presentation/shan>
- [20] Z. Wang, A. Bovik, H. Sheikh, and E. Simoncelli, "Image Quality Assessment: From Error Visibility to Structural Similarity," *IEEE Transactions on Image Processing*, vol. 13, no. 4, pp. 600–612, Apr. 2004. [Online]. Available: <http://ieeexplore.ieee.org/document/1284395/>
- [21] H.-W. Ng and S. Winkler, "A data-driven approach to cleaning large face datasets," in *2014 IEEE International Conference on Image Processing (ICIP)*. Paris, France: IEEE, Oct. 2014, pp. 343–347. [Online]. Available: <http://ieeexplore.ieee.org/document/7025068/>
- [22] L. v. d. Maaten and G. Hinton, "Visualizing Data using t-SNE," *Journal of Machine Learning Research*, vol. 9, no. Nov, pp. 2579–2605, 2008. [Online]. Available: <https://www.jmlr.org/papers/v9/vandermaaten08a.html>
- [23] G. B. Huang, M. Ramesh, T. Berg, and E. Learned-Miller, "Labeled faces in the wild: A database for studying face recognition in unconstrained environments," University of Massachusetts, Amherst, Tech. Rep. 07-49, October 2007.
- [24] N. Pinto, Z. Stone, T. Zickler, and D. Cox, "Scaling up biologically-inspired computer vision: A case study in unconstrained face recognition on facebook," in *CVPR 2011 WORKSHOPS*, Jun. 2011, pp. 35–42, ISSN: 2160-7516.